

Increasing the Energy Density and Power Ratio of a Staggered VAWT Wind Farm by using The Rotor's Diameter as a Reference

BUDHI MULIAWAN SUYITNO
Department Mechanical Engineering
Universitas Pancasila
Srengseng Sawah, Jagakarsa, Jakarta 12640
INDONESIA

REZA ABDU RAHMAN
Department Mechanical Engineering
Universitas Pancasila
Srengseng Sawah, Jagakarsa, Jakarta 12640
INDONESIA

ISMAIL
Department Mechanical Engineering
Universitas Pancasila
Srengseng Sawah, Jagakarsa, Jakarta 12640
INDONESIA

ERLANDA AUGUPTA PANE
Department Mechanical Engineering
Universitas Pancasila
Srengseng Sawah, Jagakarsa, Jakarta 12640
INDONESIA

Abstract: - The development of wind energy systems has achieved a higher technology readiness level for Horizontal Axis Wind Turbine (HAWT). Unfortunately, the HAWT is only suitable for high wind speed areas. The Vertical Axis Wind Turbine (VAWT) is considered the ideal model to utilize wind energy in the low wind speed region. However, VAWT has a lower power coefficient. Therefore, developing a VAWT wind farm can improve the overall energy density for power generation in the low wind speed region. In this study, staggered configuration for three turbine clusters is evaluated through numerical simulation and experimental tests. The pitch distance is set by using the rotor's diameter as a reference for placing the 3rd rotor at the second row. The turbulence intensity in the area wake superposition is highly affected by the position of the 3rd rotor. The flow characteristic indicates that the 3D layout has a high concentration at the front area of the 3rd rotor. It leads to higher achievement of power ratio for the clusters. The overall power ratio for 3D layout can achieve more than 0.9, whereas, at a speed 3 m/s, the highest power ratio is obtained at 1.0. The finding in this study can be set as an essential reference for developing a VAWT wind farm with a specific arrangement and improving the overall power density of the turbine clusters.

Key-Words: - Savonius rotor, Turbulence, VAWT, Wake superposition, Wind farm

Received: May 18, 2021. Revised: January 22, 2022. Accepted: February 19, 2022. Published: March 26, 2022.

1 Introduction

The energy crisis encourages researchers and designers to improve renewable energy sources' utilization continuously [1]. As a result, the growth of renewable energy sources increases rapidly, with

a positive trend in the near future. The options for storing renewable energy are enlarged by using thermal or electrical energy storage [2]–[4]. Further, advanced storage systems by indirect hydrogen production and pumped hydro storage offer better flexibility for utilizing renewable energy sources. In

recent years, wind energy development has been an excellent example of sustainable development in renewable energy [5].

High-efficiency wind turbine model Horizontal Axis Wind Turbine (HAWT) is achieved owing to massive research for improving the design of the turbine [6]. However, the HAWT turbine is limited by geographical requirement since it works ideally for an area with high wind speed. In order to utilize the wind energy for an area with low potential wind speed, the Vertical Axis Wind Turbine (VAWT) is a better option. The VAWT model is able to harvest low wind speed and produce sufficient rotational torque to produce mechanical work. The produced work can be used for generating electricity for small utilities. Therefore, the development of VAWT is highly recommended for a particular application such as lighting and pumping system [7], [8].

To improve the power output from the turbine, several wind turbines are assembled under a specified area called a wind farm. The average output of windfarm is considerably high since it employs more than one turbine and is able to improve the produced energy density [9]. Nevertheless, the layout of the turbine should be appropriately adjusted to reduce the area as well as to minimize the wake superposition effect [10]. The improper arrangement leads to low energy density and increases the processing and production cost. For example, wake superposition can be minimized by increasing the distance between the first and second-row turbine, but it increases the area's usage and eventually decreases the energy density [11]. If the turbine is set closer, the wake superposition increases and the power generation on the second-row turbine drop significantly. Besides, the layout arrangement of the wind farm has to consider the operational aspect, such as energy storage, maintenance and power distribution [12].

Numerous studies have analyzed the ideal configuration for a wind farm. Unfortunately, it focuses on the HAWT windfarm [13]. The study that addressed the VAWT wind farm layout is limited since the VAWT is only suitable for low wind speed areas with small energy production. Also, the design of VAWT is relatively complex and makes this turbine is less attractive. The complexity for VAWT is aimed at the design of the turbine and low power produced, which makes it less feasible for large-scale application [14]–[16]. Despite that, one study reports that an optimal configuration for the VAWT wind farm is able to maximize the potential energy of wind energy [17]. The study describes that with a proper turbine design and suitable layout for VAWT, low wind

speed can convert as usable energy when it is addressed for specific applications instead of large-scale electric production like HAWT. For example, an inline configuration of two VAWT can improve the power ratio up to 0.34 [18]. Another study reported that staggered configuration for VAWT wind farms with three turbine clusters could increase the overall power ratio by 0.8 [19]. Further research is still necessary for the VAWT wind farm by considering the achievement for the VAWT wind farm and the opportunity to improve its power ratio [20].

The VAWT wind farm is highly recommended to be improved by addressing suitable configuration for staggered configuration. Increasing the power ratio will improve the impact factor for windfarm VAWT in the renewable energy system and broader application. A previous study shows that by using the Myring Equation for designing the Bach-type blade for *Savonius* VAWT, a better power coefficient can be achieved [21]. Thus, the present study aims to find a suitable configuration for a VAWT wind farm in a staggered layout. The three turbine clusters are chosen and adjusted using the rotor's diameter (D) as a specific base point. By finding the ideal layout and the highest power ratio, the energy density for the VAWT wind farm can be increased significantly and make it suitable to be used as an essential reference for developing a large-scale VAWT wind farm.

2 Materials and Method

Bach-type *Savonius* rotor is used in this study. The consideration for using the given model is a better air distribution in any wind direction and relatively easy to be manufactured [22]–[24]. The curvature of the rotor was adjusted by using the Myring Equation; thus, the model can be adapted precisely [25].

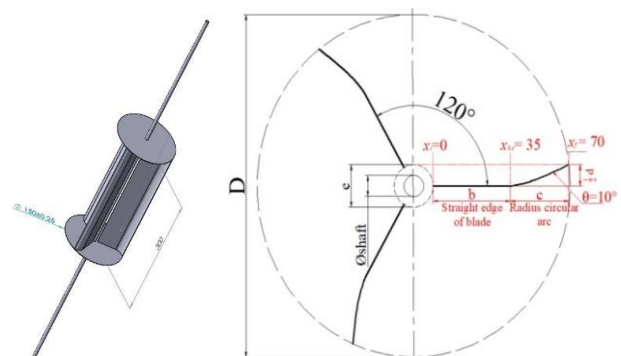


Fig. 1: The geometry of the *Savonius* turbine

The designed rotor was used the curve parameter control ($\theta = 10^\circ$) with three blades. The height and diameter of the turbine were 300 mm and 150 mm, respectively (Fig. 1).

The staggered configuration was used three turbine clusters. In order to study the effect of pitch distance between the turbine in the first and second row, the 3rd rotor was varied by taking the turbine's diameter as reference. The diameter is taken as a specific reference to refer to a specific arrangement for the designing windfarm. Fig. 2 presents the basic orientation for the layout. The measurement point at x and y were chosen since this area has the highest turbulence intensity according to the wind speed direction. An experimental test for the turbine was performed using an open-loop wind tunnel with high feasibility and reduced the deviation for the measurement [26].

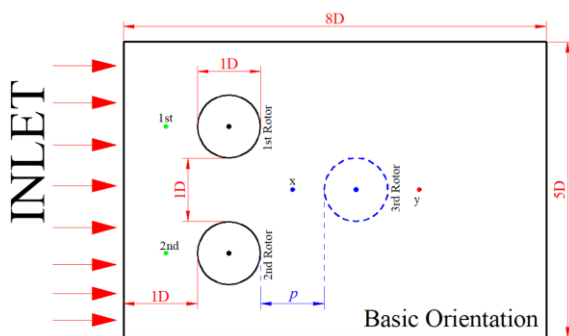


Fig. 2: Basic layout configuration and measurement at the test section

The 3rd rotor (at second row) is varied by pitch distance at $1D - 4D$. Numerical simulation using the software was conducted first to evaluate the turbulence value, power ratio, and flow characteristic at the wake superposition area. The simulation was intended to obtain the best configuration of the turbine by understanding the effect of wake superposition and turbulence on the power ratio.



Fig. 3: a) Initial measurement, b) Experimental test for best staggered configuration

The power ratio was taken as the main indicator to determine the best configuration where it is taken from the rotational speed and power generated of the turbine at the first and second row. According to the standard for low wind speed area, the wind speed for measurement is set at 1–5 m/s. One turbine prototype was used to check the readability of the instrument (Fig. 3a). The wind speed in the wind tunnel was measured using an anemometer (hot wire), where a tachometer measured the rotational speed of the turbine. The best staggered configuration (Fig. 3b) was evaluated experimentally and repeated ten times to ensure the data acquisition and minimize the deviation of measurement.

3 Results

The changes in turbulence value at the wake superposition area are mainly affected by the arrangement of the second-row turbine. Fig. 4 presents the turbulence value under different pitch configurations given wind speed (1 – 5 m/s). The turbulence value at the front area of the first-row turbine (measurement point at 1st and 2nd, as seen in Fig. 2) shows an identical value where the turbulence tends to increase along with an increment in the wind speed. However, the turbulence value at the midpoint (x) and rear (y) change significantly as the wind speed increases, related to the pitch distance between the first and second-row turbine. At pitch $1D$ and $2D$, the turbulence value at the area before the 3rd rotor (x) is always smaller than the turbulence at the rear area (y). In contrast, at positions $3D$ and $4D$, the turbulence value changes at x and shows a smaller value than turbulence at y.

In order to understand the flow pattern at the designed configuration, Fig. 5 presents the characteristic of wind speed at different configurations. The pattern is plotted at wind speed 3 m/s since it is the median value of the tested wind speed. The flow distribution at the first-row turbine presents a stable flow associated with the turbulence value in this area as the distance to the second-row turbine (3rd rotor) changes, the flow characteristic at the wake superposition area is also different. It can be seen at $1D$ that the concentration of wind speed at the front area of the 3rd rotor is high. When the 3rd rotor is moved farther from the first-row turbine, the flow characteristic at this area varies greatly. At pitch $2D$, the passing wind from the first row collides, making the velocity concentration at the front area of the 3rd rotor split. The passing wind from the first-row turbine promotes a stable flow at pitch distance $4D$ since the space between the first

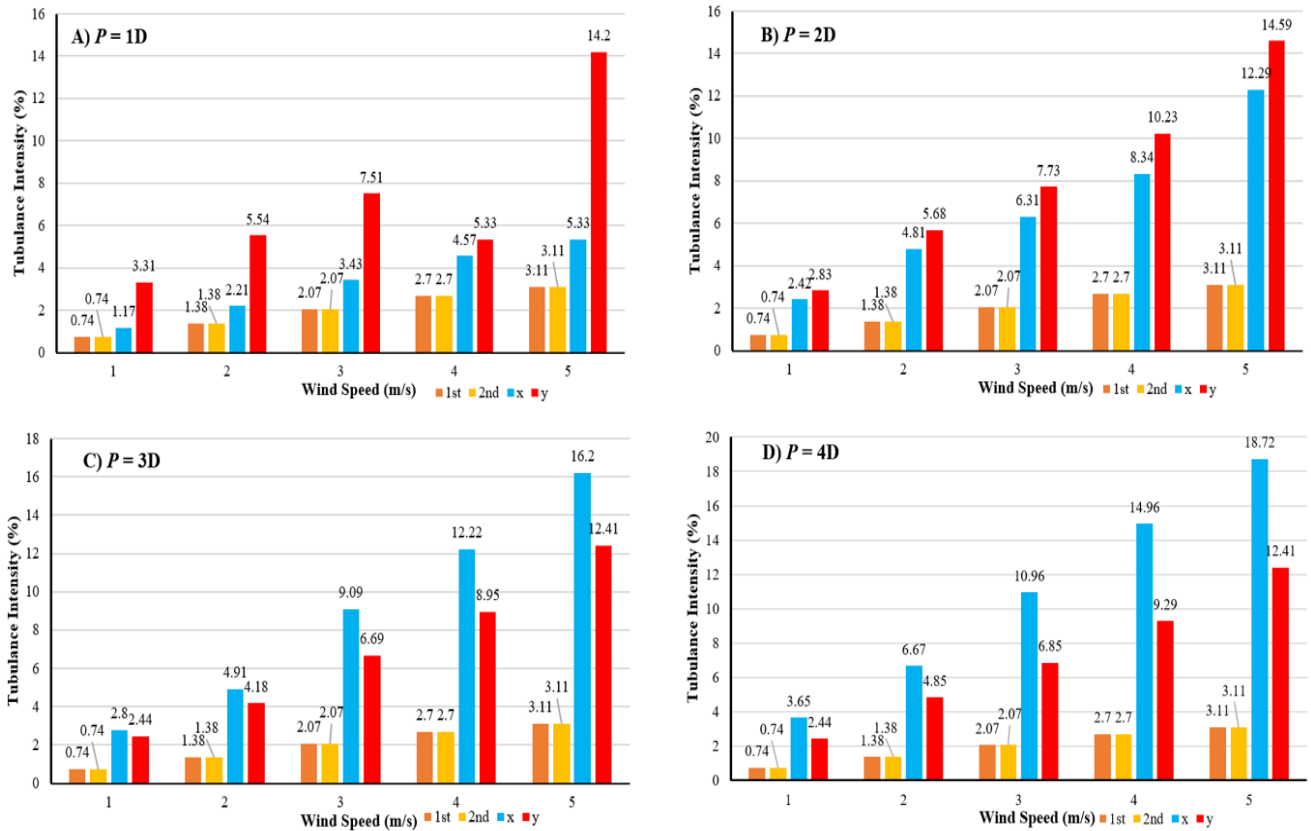


Fig. 4: Turbulence value at different configuration

and second-row turbine is far enough to achieve a laminar flow. The 3D configuration obtains the ideal flow where the passing wind from the first-row turbine is concentrated at the middle of the 3rd rotor.

The changes in the flow affect the power generated by the turbine, particularly for the second-

row turbine (3rd rotor). The power generated by the turbine gained from the simulation is analyzed to obtain the power ratio. Fig. 6 presents the power ratio comparison at different layout configurations under specific wind speeds. The lowest power ratio is found at pitch distances 1D and 4D, where the

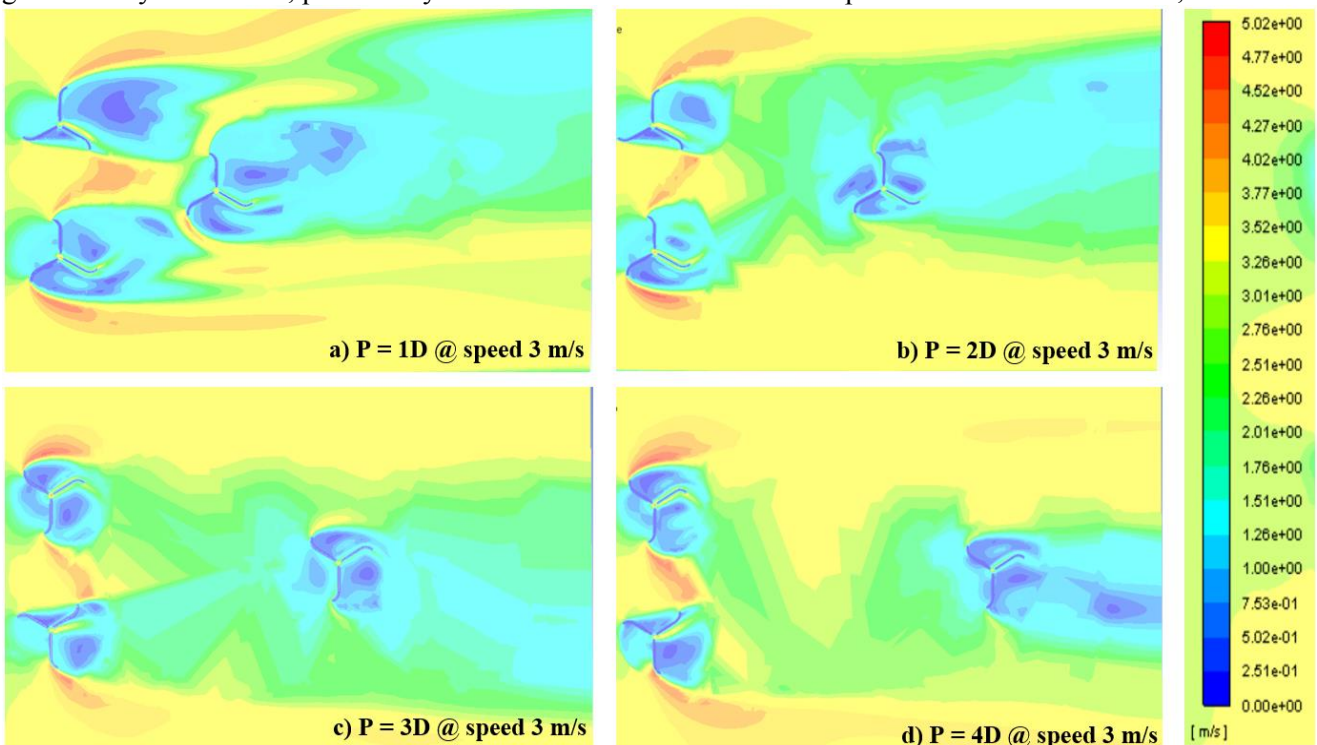


Fig. 5: Flow characteristic at different configurations with wind speed at 3 m/s

value is less than 1 at wind speed 1–5 m/s. It emphasizes that the power ratio is affected by the layout configuration of the turbine cluster. For pitch distance 1D, the short distance between the first and second-row turbine disrupts the flow after passing the first-row turbine. It makes the power generation for the second-row turbine decrease. On the contrary, a wide distance at pitch 4D reduces the flow concentration and leads to low power generation on the second-row turbine. According to the power ratio, pitch 2D and 3D show a suitable result where the power ratio at wind speed 3 m/s is more than 1. However, pitch 3D has a higher mean power ratio than pitch 2D, where most of the power ratio is more than 0.9.

According to the simulation result, pitch 3D has the highest power ratio. This layout is chosen for the experimental test to obtain the actual power ratio. The measurement is taken through a wind tunnel

a good agreement that the power ratio for 3D has the highest value.

4 Discussion

The effect of pitch distance between the first and second-row turbine is mainly on the change of turbulence intensity. It is the main reason for finding the optimal configuration to adjust the turbulence intensity around the wind farm, particularly for the second-row turbine. The increment in turbulence intensity is primarily on the area wake superposition as well as the rear area of the second-row turbine. As observed in Fig. 4, the area wake superposition and after 3rd rotor shows a high turbulence intensity. The highest turbulence intensity is obtained by pitch distance of 3D and 4D while it elevates as the wind speed increases. The turbulence intensity before and after area wake superposition also can be used to

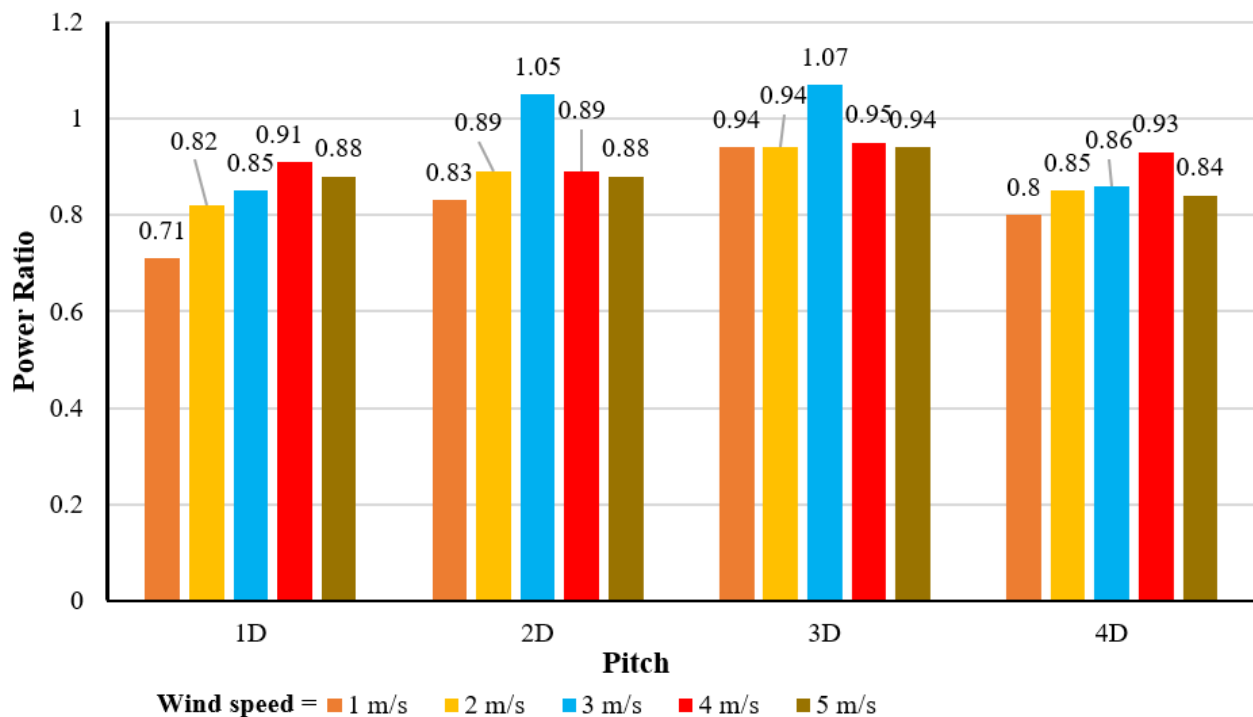


Fig. 6: The change in power ratio at different configuration

and is repeated 10 times to ensure the reliability of the measurement. The power generated on the first-row turbine is compared to the power generated on the 3rd rotor. As shown in Fig. 7, the power ratio is relatively high for the configuration 3D, with an average value of more than 0.9. the power ratio at wind speed 3 m/s is more than 1, indicating an excellent indicator of the suitable layout for staggered configuration with three turbine clusters. Also, both experimental and simulation results show

determine the ideal flow distribution on the second-row turbine. The turbulence intensity for 3D configuration decreases significantly after passing the 3rd rotor. It shows that the second-row turbine can absorb a sufficient amount of wind energy. It also can be observed by understanding the flow characteristic in this area.

The flow characteristic is plotted at wind speed 3 m/s for each layout configuration. Fig. 5 presents that pitch distance 3D indicates a high concentration flow at the front area of the 3rd rotor. It is the major

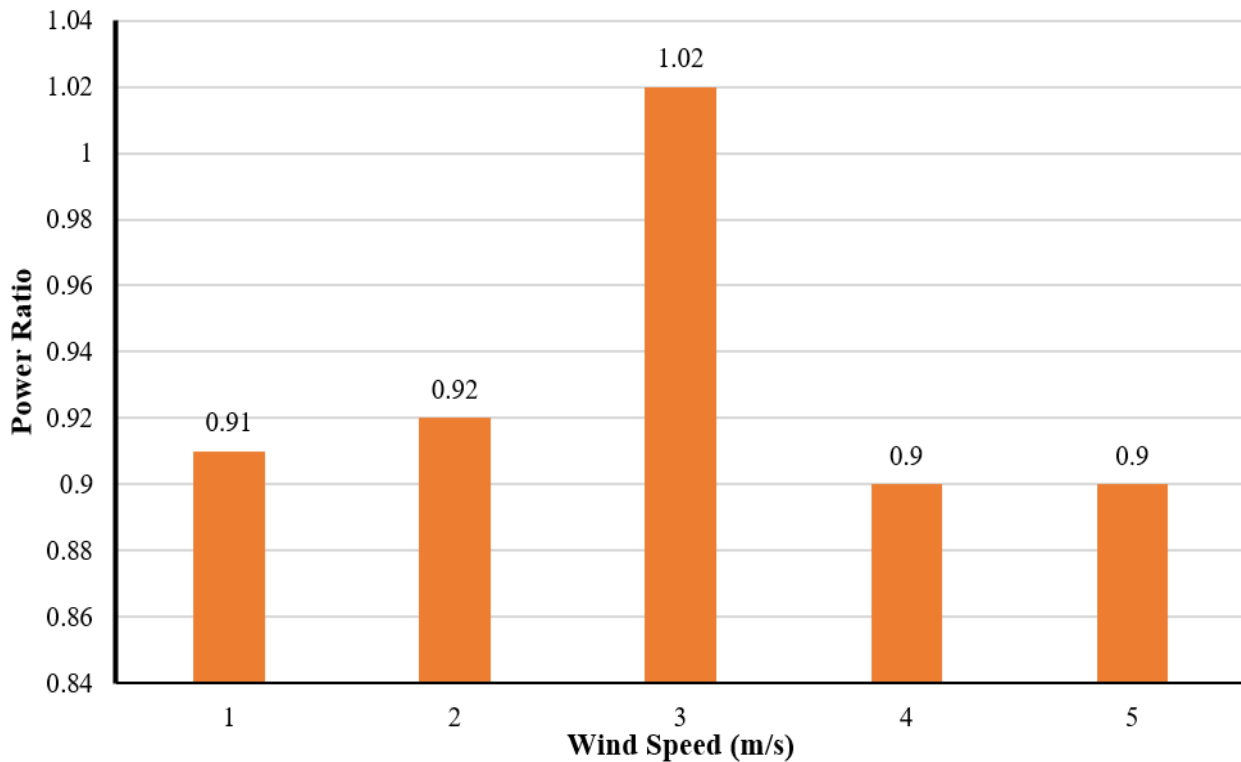


Fig. 7: Experimental result for power ration at pitch 3D

factor that leads to a high turbulence intensity at the area wake superposition for 3D configuration. A high concentration of airflow in the front of the second-row turbine leads to a significant energy conversion which can be addressed based on the differences in turbulence intensity between the area before and after 3rd rotor. The wind speed distribution is spread equally with minor degradation. It emphasizes that the turbulence intensity for 3D configuration at the area before and after the 3rd rotor slightly decreases. The finding is also supported by the previous study, which concluded that a suitable adjustment for the turbine in the first row could lead to a coupled effect for the area wake superposition and increase the power characteristic for the second-row turbine [27]. It is advantageous since the power generation for the second-row turbine could be increased and raise the power ratio of the layout configuration.

The highest power ratio is obtained for 2D and 3D layout configuration, as seen in Fig. 6. However, the average power ratio for pitch distance 2D is relatively smaller than pitch distance 3D. It is mainly affected by the wind distribution at the area wake superposition and turbulence intensity on the 2D configuration, which leads to low power generation on the second-row turbine. It points out that area wake superposition is important for wind farms with more than one-row cluster and depends

adjusting the distance between first and second-row turbines. A suitable pitch distance is able to improve the power ratio of the clusters. Also, the use of Bach-type blade for *Savonius* rotor promotes a better wind direction after passing the rotor and increases the wind concentration at the front of 3rd rotor, leading to a higher power generation for the second-row turbine [28]–[30]. The importance of adjusting the pitch distance between first and second-row turbines also can be proven by 1D and 4D layout configuration. Both configurations show a low power ratio since the pitch distance is too close (for 1D) or too wide (for 4D) and lead to a significant drop in the power ratio (less than 0.9) [31].

Experimental evaluation for 3D configuration shows a high-power ratio for the all-ranged wind speed and is relatively close to the simulation result (Fig. 7). It proves that 3D configuration is able to deliver a high-power density for the staggered VAWT wind farm. Thus, the ideal layout for a staggered VAWT wind farm can be adjusted precisely, as seen in Fig. 8. The specific area of the configuration is 3D × 6D. With a smaller area for the windfarm and a high-power ratio, the area's energy density could be improved significantly [32]. Thus, the proposed model using 3D configuration can be used to design a staggered VAWT wind farm.

5 Conclusion

A detailed study is done to find an ideal VAWT wind farm with a staggered configuration. Though VAWT is only suitable for low wind speed areas and has a lower power coefficient, by adjusting a proper layout, the overall power density of the wind farm can be utilized effectively. The change in pitch distance between the first and second-row turbine shift the turbulence intensity, particularly for the area before and after the second-row turbine. The flow characteristic of each layout is observed and emphasized the turbulence intensity for each model. The pitch distance 3D shows a better turbulence intensity with a fair distribution of wind speed in the area wake superposition. It increases the power generated for the second-row turbine (3rd rotor). Thus, the power ratio obtained from the power generation between the first and second-row turbine shows a higher value for the 3D configuration. Both results from the experiment and simulation indicate a high-power ratio for 3D configuration. The average power ratio is obtained more than 0.9 where at wind speed 3 m/s, the power ratio is able to achieve value by 1.02. The proposed layout in this study can be referred for further improvement in the VAWT wind farm and is expected to increase the technology readiness level for wind power generation with VAWT.

References:

- [1] R. A. Rahman, A. Suwandi, and M. Nurtanto, "Experimental investigation on the effect of thermophysical properties of a heat transfer fluid on pumping performance for a convective heat transfer system," *J. Therm. Eng.*, vol. 7, no. 7, pp. 1628–1639, 2021.
- [2] D. Rahmalina, D. C. Adhitya, R. A. Rahman, and I. Ismail, "Improvement the Performance of Composite Pcm Paraffin-Based Incorporate With Volcanic Ash As Heat Storage for Low-Temperature," *EUREKA Phys. Eng.*, no. 1, pp. 3–11, 2022.
- [3] D. Rahmalina, R. A. Rahman, and Ismail, "Increasing the rating performance of paraffin up to 5000 cycles for active latent heat storage by adding high-density polyethylene to form shape-stabilized phase change material," *J. Energy Storage*, vol. 46, no. December 2021, p. 103762, 2022.
- [4] D. Rahmalina, R. A. Rahman, and I. Ismail, "Improving the phase transition characteristic and latent heat storage efficiency by forming polymer-based shape-stabilized PCM for active latent storage system," *Case Stud. Therm. Eng.*, p. 101840, 2022.
- [5] Renewable Costs in 2017 Generation Power, *Renewable Power Generation Costs in 2017*. 2018.
- [6] B. A. Storti, J. J. Dorella, N. D. Roman, I. Peralta, and A. E. Albanesi, "Improving the efficiency of a Savonius wind turbine by designing a set of deflector plates with a metamodel-based optimization approach," *Energy*, vol. 186, p. 115814, 2019.
- [7] B. Hand and A. Cashman, "Aerodynamic modeling methods for a large-scale vertical axis wind turbine: A comparative study," *Renew. Energy*, vol. 129, pp. 12–31, 2018.
- [8] Z. Tasneem *et al.*, "An analytical review on the evaluation of wind resource and wind turbine for urban application: Prospect and challenges," *Dev. Built Environ.*, vol. 4, p. 100033, 2020.
- [9] J. F. Cao, W. J. Zhu, W. Z. Shen, J. N. Sørensen, and Z. Y. Sun, "Optimizing wind energy conversion efficiency with respect to noise: A study on multi-criteria wind farm layout design," *Renew. Energy*, vol. 159, pp. 468–485, 2020.
- [10] Z. Ti, X. W. Deng, and H. Yang, "Wake modeling of wind turbines using machine learning," *Appl. Energy*, vol. 257, p. 114025, 2020.
- [11] G. Aquila, L. C. Souza Rocha, P. Rotela Junior, J. Y. Saab Junior, J. de Sá Brasil Lima, and P. P. Balestrassi, "Economic planning of wind farms from a NBI-RSM-DEA multiobjective programming," *Renew. Energy*, vol. 158, pp. 628–641, 2020.
- [12] M. Naemi and M. J. Brear, "A hierarchical, physical and data-driven approach to wind farm modelling," *Renew. Energy*, vol. 162, pp. 1195–1207, 2020.
- [13] F. Liu, J. Ma, W. Zhang, and M. Wu, "A comprehensive survey of accurate and efficient aggregation modeling for high penetration of large-scale wind farms in smart grid," *Appl. Sci.*, vol. 9, no. 4, 2019.
- [14] H. F. Lam and H. Y. Peng, "Development of a wake model for Darrieus-type straight-bladed vertical axis wind turbines and its application to micro-siting problems," *Renew. Energy*, vol. 114, pp. 830–842, 2017.
- [15] E. Antar and M. Elkhoury, "Parametric sizing optimization process of a casing for a Savonius Vertical Axis Wind Turbine," *Renew. Energy*, vol. 136, pp. 127–138, 2019.
- [16] P. K. Talukdar, A. Sardar, V. Kulkarni, and

- U. K. Saha, "Parametric analysis of model Savonius hydrokinetic turbines through experimental and computational investigations," *Energy Convers. Manag.*, vol. 158, no. December 2017, pp. 36–49, 2018.
- [17] A. Vergaerde *et al.*, "Experimental characterisation of the wake behind paired vertical-axis wind turbines," *J. Wind Eng. Ind. Aerodyn.*, vol. 206, no. July, p. 104353, 2020.
- [18] I. Ismail, R. A. Rahman, G. Haryanto, and E. A. Pane, "The Optimal Pitch Distance for Maximizing the Power Ratio for Savonius Turbine on Inline Configuration," *Int. J. Renew. Energy Res.*, vol. 11, no. 2, pp. 595–599, 2021.
- [19] A. Barnes and B. Hughes, "Determining the impact of VAWT farm configurations on power output," *Renew. Energy*, vol. 143, pp. 1111–1120, 2019.
- [20] J. Liu, H. Lin, and J. Zhang, "Review on the technical perspectives and commercial viability of vertical axis wind turbines," *Ocean Eng.*, vol. 182, no. April, pp. 608–626, 2019.
- [21] I. Ismail, E. A. Pane, G. Haryanto, T. Okviyanto, and R. A. Rahman, "A Better Approach for Modified Bach-Type Savonius Turbine Optimization," *Int. Rev. Aerosp. Eng.*, vol. 14, no. 3, p. 159, 2021.
- [22] B. A. Storti, J. J. Dorella, N. D. Roman, I. Peralta, and A. E. Albanesi, "Improving the efficiency of a Savonius wind turbine by designing a set of deflector plates with a metamodel-based optimization approach," *Energy*, vol. 186, p. 115814, 2019.
- [23] A. Ramadan, K. Yousef, M. Said, and M. H. Mohamed, "Shape optimization and experimental validation of a drag vertical axis wind turbine," *Energy*, vol. 151, pp. 839–853, 2018.
- [24] M. Saleh and F. Szodrai, "Numerical Model Analysis of Myring–Savonius wind turbines," *Int. J. Eng. Manag. Sci.*, vol. 4, no. 1, pp. 180–185, 2019.
- [25] Y. hang Hou, X. Liang, and X. yang Mu, "AUV hull lines optimization with uncertainty parameters based on six sigma reliability design," *Int. J. Nav. Archit. Ocean Eng.*, vol. 10, no. 4, pp. 499–507, 2018.
- [26] Ismail, J. John, E. A. Pane, R. Maulana, R. A. Rahman, and A. Suwandi, "Experimental evaluation for the feasibility of test chamber in the open-loop wind tunnel," *WSEAS Trans. Fluid Mech.*, vol. 16, pp. 120–126, 2021.
- [27] A. Posa, "Wake characterization of coupled configurations of vertical axis wind turbines using Large Eddy Simulation," *Int. J. Heat Fluid Flow*, vol. 75, no. November 2018, pp. 27–43, 2019.
- [28] H. Bai and C. Chun-Man, "Positive interactions of two Savonius-type vertical-axis wind turbines for performance improvement," *Energy Procedia*, vol. 158, pp. 625–630, 2019.
- [29] K. Kacprzak, G. Liskiewicz, and K. Sobczak, "Numerical investigation of conventional and modified Savonius wind turbines," *Renew. Energy*, vol. 60, pp. 578–585, 2013.
- [30] T. C. Hohman, L. Martinelli, and A. J. Smits, "The effect of blade geometry on the structure of vertical axis wind turbine wakes," *J. Wind Eng. Ind. Aerodyn.*, vol. 207, no. April 2019, p. 104328, 2020.
- [31] S. Shaaban, A. Albatal, and M. H. Mohamed, "Optimization of H-Rotor Darrieus turbines' mutual interaction in staggered arrangements," *Renew. Energy*, vol. 125, pp. 87–99, 2018.
- [32] S. ho Hur, "Reliable and cost-effective wind farm control strategy for offshore wind turbines," *Renew. Energy*, vol. 163, pp. 1265–1276, 2021.

Contribution of Individual Authors to the Creation of a Scientific Article (Ghostwriting Policy)

Budhi Muliawan Suyitno: Conceptualization and methodology

Reza Abdu Rahman: Writing and visualization

Ismail: Formal analysis and supervision

Erlanda Augupta Pane: Data acquisition and investigation

Creative Commons Attribution License 4.0 (Attribution 4.0 International, CC BY 4.0)

This article is published under the terms of the Creative Commons Attribution License 4.0

https://creativecommons.org/licenses/by/4.0/deed.en_US